International Research Journal of Innovations in Engineering and Technology (IRJIET)

ISSN (online): 2581-3048
Volume 9, Issue 6, pp 42-62, June-2025
https://doi.org/10.47001/IRJIET/2025.906007

Studying Effect of Activation Energy and Chemical Reaction with Heat and Mass Transfer of Maxwell Fluid on Riga Plate Embedded in Porous Media

[1]*Shyam Manohar Suthar, [2]Dr. Shweta Bohra

[1,2]Department of Mathematics, Sangam University, Bhilwara, Rajasthan, 311001, India
*Corresponding Author's E-Mail: tabletst9@gmail.com

Abstract **- This present article delves the behavior of a Maxwell fluid flow over a Riga plate nestled in a porous media, examining chemical reactions, activation energy, coupled with heat and mass transfer simultaneously. The governing system of highly coupled, nonlinear PDEs is transformed into a set of ODEs through suitable application of similarity transformations. Accuracy in the solving of the resulting system of ODEs was achieved through the application of the Bvp4c solver in MATLAB. A thorough parametric study has been performed to check the influences of different physical quantities such as Deborah number, porosity number, modified Hartmann number, thermal and mass Grashof numbers, velocity slip parameter, Stefan-Boltzmann coefficient, Prandtl number, radiation parameter, thermophoresis & Brownian motion parameter, Eckert number, Schmidt number, chemical reaction parameter, temperature difference parameter, and activation energy, suction/injection coefficient, and concentration slip parameter. The velocity, temperature, and concentration profiles effected by these parameters are extensively analyzed graphically and through tabulated data. The results serve as a basis for understanding the control mechanisms for non-Newtonian fluid flows in engineering and industrial processes involving porous media and electromagnetic fields.**

Keywords: Riga Plate, Maxwell Fluid, Porus Media, Heat & Mass Transfer, Chemical Reaction, Activation Energy.

I. INTRODUCTION

The Riga plate is fine-tuned artificial electromagnetic surface construct designed to manipulate boundary layer properties and control fluid flow characteristics especially in weakly hydromagnetic fluids. Invented by Gailitis and Lielausis in 1991 [1], the Riga plate (Electromagnetic Activator) has electrodes and magnets alternately arranged along-the surface, whereby their activation creates a "Lorentz force" that runs parallel to the wall in such a way it affects the fluid motion, thereby creating electromagnetic hydrodynamic behavior. Normally, a Riga plate is observed as flat, having organized distributions of magnets and electrodes lying underneath. The applications of a Riga plate would include aerodynamics, industrial processes, and heat transfer operations, where precision in flow control is required. Recent research has focused on investigating other effects on fluid flow over a Riga Plate such as melting heat, thermal radiation, and viscous dissipation in order to improve performance and understanding of the system.

Non-Newtonian fluids have extraordinary properties in that they demonstrate non-constant viscosity. Viscosity is dependent on the shear stress or strain rate applied. Such behavior does not conform to Newton's classical laws of viscosity. Unlike Newtonian fluids, which have a linear relationship between shear stress and strain, these non-Newtonian fluids exhibit interesting effects, including shear-thinning, shear-thickening, and sometimes altering into a solid state when subjected to sudden shock. Their importance can be warranted in fields ranging from the design of shear-thickening fluids for making bullet-proof vests through advanced medical appliances, cosmetics, and food processing up to cutting-edge construction materials that mitigate vibrations. A noteworthy example of non-Newtonian behavior is the Maxwell fluid, put forth by James Clerk Maxwell in 1867. He introduced this fluid with the aim to cast understanding on the viscous and elastic behaviors related to gases and molecular motions. His initiatives laid the very foundations for the viscoelastic theory, and nowadays Maxwell fluids are vital for simulating the behavior of several complex materials such as polymer melts, biological tissues, and some industrial lubricants, therefore advancing engineering, biomedicine, and material sciences.Activation energy is the inherent characteristic of chemical kinetics that finds its place as the minimum energy barrier to start a chemical reaction. It is, thus, a vital parameter to decide how fast a reaction occurs, through that degree of free energy required for reactants to transform under an ambient condition. Alongside chemical reactions, the principles of heat and mass transfer that describe the mechanism of heat and mass movement through different media are essential for optimizing industrial processes, from chemical reactors to energy

ISSN (online): 2581-3048
Volume 9, Issue 6, pp 42-62, June-2025
https://doi.org/10.47001/IRJIET/2025.906007

systems. Controlling these transfers is necessary in guaranteeing the efficiency, safety, and sustainability of such processes as distillation, drying, and thermal control in electronics. Another important area of investigation is that of porous media, where the main subject consists of materials that contain voids or pores interconnected by a network of channels extending through the material body. The role of porous structures is paramount in controlling the transport processes of heat, mass, and fluids, and thus govern applications such as groundwater remediation, oil recovery, or drug delivery systems. In unison, all these activation-energy concepts, heat and mass moves, and porous media exist at the heart of thousands of technological advances that fuel the new frontiers of energy, health care, environmental management, and advanced manufacturing.

Loganathan et al. [2] done their analysis of heat and mass transfer on Casson fluid over a permeable riga plate and they found that Thermal conductivity is crucial for heat transfer and influences other flow properties. This study focuses on how temperature-dependent thermal conductivity affects Casson fluid flow over a Riga plate.Later, Adeosun et al. [3]worked on Casson nanofluid over a melting riga plate with porous media and they concluded modified Hartman number and melting parameters generally enhance velocity, while Casson and thermophoresis parameters impact nanoparticle concentration. Heat and mass transfer rates, indicated by Nusselt and Sherwood numbers, are strongly affected by variations in these physical parameters. After Adeosun, Sindhu et al. [4]scrutinized Comparative analysis of darcy–forchheimer radiative flow of a water-based Al2O3-Ag/TiO2 hybrid nanofluid over a riga plate with heat sink/source. Vijayalakshmi et al. [5]investigate Effect of chemical reaction and activation energy on Riga plate embedded in a permeable medium over a Maxwell fluid flow and conclude that increasing the MHD parameter reduced velocity but raised both temperature and concentration profiles, while higher radiation, Eckert number, Biot number, and activation energy also enhanced temperature and concentration. However, increasing the Prandtl number, chemical reaction rate, and Schmidt number (Sc) led to decreases in temperature and concentration profiles. The importance of the chemical reaction with activation energy involved in the Riga wedge flow of tangent hyperbolic nanofluid in the presence of a heat source has been evaluated by Abdal et al.[6]. Khatun et al. [7] performed numerical investigation of electro-magnetohydrodynamic (EMHD) radiating fluid flow nature along an infinitely long vertical Riga plate with suction in a rotating system. Higher-order endothermic/exothermic reactions with activation energy that considers the effect of thermophoresis and Brownian motion on mixed convective flow with magnetic fields across a vertically stretching surface depicted by Sharma et al. [8]. Raju et al. [9]inspected under equilibrium conditions, how activation energy and chemical reactions affect Maxwell fluid flow. It is found that the reversible flows possess thinner concentration boundary layers than those of irreversible flows, which enhances heat and mass transfer rates and is significant for design applications such as heat exchangers and reactors. Reaction rates and selectivity are given by using sulphuric acid as a catalyst with Maxwell fluid, and this facilitates an accurate design of the catalytic process. The impact of activation energy and variable properties on peristaltic flow through a porous wall channel discussed by Rafiq et al.[10].Mathematical analysis of heat and mass transfer in an unsteady stagnation-point flow over a Riga plate with binary chemical reactions and thermal radiation effects perused by Khan et al. [11]. Parvine et al. [12] focused on EMHD nanofluid flow along a porous riga plate with thermal radiation. Loganathan et al. [13]manifested Ree-Eyring nanofluid dynamics over a convection-heated Riga plate, considering effects like free convection, bioconvection, heat source, and thermal radiation. Bioconvection due to motile microorganisms and factors like thermophoresis and Brownian motion are analyzed. An unsteady magnetic hydrodynamic flow of a Maxwell nano liquid in the presence of nonlinear thermal radiation is impacted by chemical reaction over a porous vertical sheet scrutinized by Ali et al.[14]. Abdal et al. [15] presented a paper on magnetohydrodynamic stretched flow of Williamson Maxwell nanofluid through porous matrix over a permeated sheet with bioconvection and activation energy and their finding indicate that enhancing the magnetic parameter M, the velocity of fluid decreases but opposite behavior happens for temperature, concentration and motile density profile. Also, the motile density profile decreases down for Pe and Lb. The skin friction coefficient is enhanced for both the Williamson and Maxwell fluid.Later, Ishtiaq et al.[16] conducted a study on 2-D unsteady flow of Maxwell fluid over a vertical Riga plate under radiative effects. Effect of Gyrotactic Microorganisms on Williamson fluid Flow Past an Exponential Moving Plate with Pseudoplasticity explored by Waqas et al. [17]. Over horizontal channel effects of activation energy and chemical reaction on unsteady MHD dissipative Darcy–Forchheimer squeezed flow of Casson fluid examined by Li et al. [18] and conclude that Fluid velocity and temperature were found to increase as the plate distances tighten. Furthermore, the rise in the Hartmann number was correlated with decreasing fluid velocity due to considerable Lorentz forces. Due to Brownian motion, temperature and the concentration of the liquid rise. These increase in the parameters of Darcy–Forchheimer and activation energy will decrease the velocity and concentration. Sudarmozhi et al. [19] performed double diffusion in a porous medium of MHD Maxwell fluid with thermal radiation, heat generation and chemical reaction.

International Research Journal of Innovations in Engineering and Technology (IRJIET)

ISSN (online): 2581-3048

Volume 9, Issue 6, pp 42-62, June-2025

https://doi.org/10.47001/IRJIET/2025.906007

A numerical investigation is made for hydromagnetic heat and mass transfer by Gyrotactic microorganism flow of nanofluid over a Riga plate with chemical reaction and convective condition effects probed by Nazeer et al. [20]. The parametric study that tells us that the flow properties of the wall shear stress on the Riga plate and the motion of microorganisms are affected by the magnetic parameter and other dimensionless quantities. The melting heat effect in magnetohydrodynamics flow of a Maxwell fluid with zero mass flux studied by Ramar et al. [21]. Interesting concepts regarding transfers in heat have thus been studied in bioconvected tangent hyperbolic nanofluid flow with activation energy and Joule heating due to the Riga plate carried out by Ramasekhar et al. [22]. Sudarmozhi et al.[23] discussed Effect of heat generation and activation energy on MHD maxwell fluid with multiple slips and found that the concentration profile declines with an increase in the power index, whereas an increase in activation energy brings about an increase in this profile. Another significant finding from this research was a substantial decrease in the concentration profile when the activation energy parameter was increased. Recently, Alt et al. [24] researched about Darcy–Forchheimer nanofluid flow with thermal and solutal effects over a Riga plate and observed that The decreasing percentage of Nusselt number results when the thermal stratification varies from 0.0 to 6.0, and the decreasing percentage of Sherwood number is obtained when the solution stratification parameter varies from 0.0 to 0.6 for Williamson fluids. After, Ali Thermal-hydrodynamic analysis of a Maxwell fluid with controlled heat/mass transfer over a Riga plate: A numerical study with engineering applications explored by Alrihieli et al. [25] and The findings illustrate that by increasing the Hartmann number and simultaneously reducing the porousness and slip velocity parameters, one achieves a high velocity distribution in the case of a Maxwell fluid. These effects pointed out in the study represent the main physical discoveries on increased electromagnetic control and reduced flow resistance in the system.

Much work has been published about heat and mass transfer characteristics of non-Newtonian fluids, especially Maxwell fluids, influenced by thermal and solutal effects, magnetic fields, and porous medium. The provision of Riga plate has also evoked substantial publicity because it has realistic applications in flow control and electromagnetic actuation. Earlier studies dealt with chemical reactions, activation energy, and the influence of several boundary conditions. Still, an integrated study on the instant impact of activation energy with chemical reaction effect on the flow of Maxwell fluid over Riga plate, particularly when sandwiched inside a porous medium where heat and mass are transferred, is lacking. Such gaps pave ways for the current study to seek answers to the following key questions:

- How is activation energy important to the rate of chemical reactions in Maxwell fluid flow on a Riga plate?
- What is the coupled effect of thermal radiation, magnetic field, and porous medium on heat and mass transfer in such a system?
- What effect does the combination of those parameters have on the rheological properties of Maxwell fluid?

All these will be thereof studied to understand more about complex behaviour of fluids relevant to industries, engineering practices and beyond.

II. MATHEMATICAL PROBLEM FORMULATION

A two-dimensional steady boundary layer flow of an incompressible Maxwell fluid impinges on a nonlinear electrically conducting horizontal Riga plate. The plate is placed in a porous medium and experiences heat and mass transfer. The coordinate system is taken such that the x-axis is along the plate surface and the y-axis is normal to it. The flow is subjected to thermal radiation, chemical reaction with activation energy, and resistance of a porous medium.

Let u and v denote the velocity components along the x- and y-directions, respectively. The velocity of the Riga plate is defined as$u_w(x)$, a function of the axial coordinate. The surface temperature and concentration are T_w and C_w, while their respective ambient values are $T_\infty$and C_∞, with the assumption that $T_w > T_\infty$ and $C_w > C_\infty$. Formulation of the problem includes all effects of electromagnetic forcing through the Riga plate, porous drag, and nonlinear thermal and solutal diffusion. The boundary has imposed slip conditions on velocity due to the microstructural fluid properties.

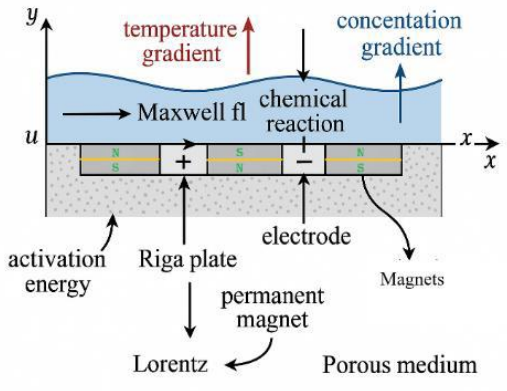

Figure 1: Riga Plate withflow Model

The main equations for mass, momentum, energy, and species concentration conservations under thermal radiation and activation energy are developed under the boundary layer. These partial differential equations in dimensional form are expressed as follows:

International Research Journal of Innovations in Engineering and Technology (IRJIET)
ISSN (online): 2581-3048
Volume 9, Issue 6, pp 42-62, June-2025
https://doi.org/10.47001/IRJIET/2025.906007

Continuity Equation:

$$\frac{\partial u}{\partial x}+\frac{\partial v}{\partial y}=0 \qquad (1)$$

Momentum Equation:

$$u\frac{\partial u}{\partial x}+v\frac{\partial u}{\partial y}+\lambda\left[u^2\frac{\partial^2 u}{\partial x^2}+v^2\frac{\partial^2 u}{\partial y^2}+2uv\frac{\partial^2 u}{\partial x\partial y}\right]$$

$$=\frac{\mu}{\rho}\frac{\partial^2 u}{\partial y^2}-\frac{\nu}{\kappa_1}u-\frac{\pi J_0 M_0 e^{\left(-\frac{\pi y}{a}\right)}}{8\rho}+g\beta'(T-T_\infty)+g\beta^*(C-C_\infty) \qquad (2)$$

Temperature Equation:

$$u\frac{\partial T}{\partial x}+v\frac{\partial T}{\partial y}=\frac{\kappa^*}{\rho C_p}\frac{\partial^2 T}{\partial y^2}+\frac{16\sigma T_\infty^3}{3k\rho C_p}\left(\frac{\partial^2 T}{\partial y^2}\right)+\tau\left[-D_B\frac{\partial C}{\partial y}\frac{\partial T}{\partial y}+\frac{D_T}{T_\infty}\left(\frac{\partial T}{\partial y}\right)^2\right]+\frac{\mu}{\rho C_p}\left(\frac{\partial u}{\partial y}\right)^2 \qquad (3)$$

Mass Equation:

$$u\frac{\partial C}{\partial x}+v\frac{\partial C}{\partial x}=D_B\left(\frac{\partial^2 C}{\partial y^2}\right)-k_c(C-C_\infty)\left(\frac{T}{T_\infty}\right)^n e^{\left(-\frac{E_c}{\kappa T}\right)}+\frac{D_T}{T_\infty}\left(\frac{\partial^2 T}{\partial y^2}\right) \qquad (4)$$

In momentum equation LHS part's first and second term u and v represent velocity of fluid in x and y direction respectively. The third term shows dimensional form of Maxwell term. In RHS first term μ and ρ represent viscosity and density of fluid, second term is recognizing as porous media, third term for riga plate, fourth and fifth term is for thermal and mass. In temperature equation ρc_p is nothing but heat capacity, second term denoted radiation term and third term shows diffusion term of mass and thermophoretic. In mass equation fluid concentration is denoted by C, chemical reaction parameter k_c, D_B is mass diffusion and second term is known as activation energy.

The appropriate boundary condition for flow, temperature and concentration is:

$$\text{At } y=0\begin{cases}u=u_w+L_1\frac{\partial u}{\partial y}\\ v=-v_w\\ T=T_w+L_2\frac{\partial T}{\partial y}\\ C=C_w+L_3\frac{\partial C}{\partial y}\end{cases}\text{ and at}y=\infty\begin{cases}u=0\\ v=0\\ T=0\\ C=0\end{cases} \qquad (5)$$

Similarity variables and non-dimensional quantities:

$$u=cxf'(\eta),\ v=-\sqrt{c\nu}\,f(\eta),\ \eta=\sqrt{\frac{c}{\nu}}\,y,\ \theta(\eta)=\frac{T-T_\infty}{T_w-T_\infty},\ \phi(\eta)=\frac{C-C_\infty}{C_w-C_\infty} \qquad (6)$$

Using these dimensionless quantities and variables we convert our dimensional equations (1)-(5) into dimensionless equations& boundary conditions (7)-(10) which presented below:

$$f'''-Kf'(\eta)-Hae^{-d\eta}+Gr\,\theta(\eta)+Gc\,\phi(\eta)-f'^2(\eta)+f(\eta)f''(\eta)+De\,(2f(\eta)f'(\eta)f''(\eta)-f^2(\eta)f'''(\eta))=0 \qquad (7)$$

$$\frac{\theta''(\eta)}{Pr}\left(1+\frac{4}{3}Rd\right)+f(\eta)\theta'(\eta)-Nb\phi'(\eta)\theta'(\eta)+Nt\theta'^2(\eta)+Ecf''^2(\eta)=0 \qquad (8)$$

$$\phi''(\eta)+Scf(\eta)\phi'(\eta)-Sc\,\sigma^*(1+d_t\theta)^n\phi(\eta)e^{\left(\frac{-E}{1+d_t\theta}\right)}+\frac{Nt}{Nb}\theta''(\eta)=0 \qquad (9)$$

International Research Journal of Innovations in Engineering and Technology (IRJIET)

ISSN (online): 2581-3048

Volume 9, Issue 6, pp 42-62, June-2025

https://doi.org/10.47001/IRJIET/2025.906007

The non-dimensional boundary conditions are:

$$\text{When } \eta \to 0 \begin{cases} f'(\eta) = 1 + \lambda_1 f''(\eta) \\ f(\eta) = s \\ \theta(\eta) = 1 + \lambda_2 \theta'(\eta) \\ \phi(\eta) = 1 + \lambda_3 \phi'(\eta) \end{cases}$$

$$\text{and for } \eta \to \infty \begin{cases} f'(\eta) = 0 \\ \theta(\eta) = 0 \\ \phi(\eta) = 0 \end{cases} \quad (10)$$

The subsequent parameter's value will be included in the nomenclature.

These physical quantities took area of interest:

- The local skin friction coefficient $C_f = \frac{\tau_w}{(\rho u_w^2)}$
- The local Nusselt number $Nu_x = \frac{x q_w(x)}{\kappa(T_w - T_\infty)}$
- The local Sherwood number $Sh_x = \frac{x q_m(x)}{D_B(C_w - C_\infty)}$

After solving given local number we achieve these results:

$\frac{1}{2} C_f \sqrt{R_e} = f''(0), \frac{Nu}{\sqrt{Re}} = -\left(1 + \frac{4}{3} Rd\right) \theta'(0), \frac{Sh}{\sqrt{Re}} = -\phi'(0).$

III. COMPUTATIONAL METHOD

Bvp4c is a MATLAB toolbox intended to solve two-point BVPs for systems of nonlinear ODEs. It is used for the interactive parametric sensitivity analysis of the optimization process. Thermal energy systems and numerous other engineering problems are also solved, as the solutions proved to be efficient. The given toolbox is integrated in the MATLAB Differential Equations Toolbox. We programmed our non-dimensional equations & boundary condition (7)-(10) in MATLAB using Bvp4c method. The value of following parameters considers as standard value:

$De = 0.2$, $K = 1$, $Ha = 0.2$, $d = 1.2$, $Gr = Gc = 0.2$, $Pr = 2$, $Rd = 0.1$, $Nt = Nb = 0.5$, $Ec = 0.2$, $Sc = 0.8$, $\sigma^* = H = 0.1$, $d_t = dt = 0.5$, $E = 0.1$, $n = 1$,$\lambda_1 = l1 = 0.1$, $\lambda_2 = l2 = 0.1$, $\lambda_3 = l3 = 0.1$ and $s = 0.2$.

Let consider $f = f(1)$, $f' = f(2)$, $f'' = f(3)$, $\theta = f(4)$, $\theta' = f(5)$, $\phi = f(6)$ and $\phi' = f(7)$.

The equations in programming are:

$$f' = f(2)$$

$$f'' = f(3)$$

$$f''' = ((1)/(1 - (De * (f(1))^2))) * ((K * f(2)) + (Ha * (\exp(-d * (eta))))) - (Gr * f(4)) - (Gc * f(6)) + ((f(2))^2) - (f(1) * f(3)) - (2 * De * f(1) * f(2) * f(3)))$$

$$\theta' = f(5)$$

$$\theta'' = (3/(3 + (4 * Rd))) * ((Pr * Nb * f(5) * f(7)) - (Pr * f(1) * f(5)) - (Nt * Pr * ((f(5))^2)) - (Pr * Ec * ((f(3))^2)))$$

$$\phi' = f(7)$$

$$\phi'' = (Sc * H * (((1 + (dt * f(4)))\hat{}n)) * f(6) * (exp(-E/(1 + (dt * f(4)))))) - (Sc * f(1) * f(7)) - ((Nt)/(Nb) * \theta''$$

International Research Journal of Innovations in Engineering and Technology (IRJIET)

ISSN (online): 2581-3048

Volume 9, Issue 6, pp 42-62, June-2025

https://doi.org/10.47001/IRJIET/2025.906007

And the non-dimensional boundary condition demonstrates as:(0 when $\eta = 0$ and inf when $\eta = \infty$)

$$\eta \to 0 \quad \begin{cases} f0(1) = s \\ f0(2) = 1 + (l1 * f0(3)) \\ f0(4) = 1 + (l2 * f0(5)) \\ f0(6) = 1 + (l3 * f0(7)) \end{cases}$$

$$\eta \to \infty \quad \begin{cases} finf(2) = 0 \\ finf(4) = 0 \\ finf(6) = 0 \end{cases}$$

IV. DISCUSSION THROUGH RESULTS

This section is root of our research work where the effects of numerous parameters on velocity, temperature and concentration of Maxwell fluid demonstrate graphically and analyzed.De (Deborah Number), K (Porosity Number), Ha (Modified Hartmann Number), Gr (Thermal Grashof Number), Gc (Mass Grashof Number), d (Electrode's width and the magnets), Pr (Prandtl Number), Rd (Radiation Parameter), Nt (thermophoresis parameter), Nb (brownian motion parameter), Ec (Eckert Number), Sc (Schmidt number), σ^* (Chemical reaction parameter), d_t(Temperature difference), E (Activation Energy), s (suction/injection coefficient),λ_1 (Velocity slip parameter), λ_2 (thermal slip parameter), λ_3 (concentration slip parameter) are those parameter which will discussed by us.

Table 1 and figure 2(a)-2(b) shows comparative study between our work and Vijayalakshmi et al. [5]'s work. Provided table clearly validate numerical value of $f''(0)$for different values of De, Ha and $d$simultaneously graphs also validate through demonstration.

Table 1: Validation of Vijayalakshmi et al. [5] same base values $\kappa = 0$, $Gr = 0$, $Gc = 0$, $\lambda_1 = 0$, $\lambda_2 = 0$, $\lambda_3 = 0$, $s = 0$

Effect of following Parameter			Vijayalakshmi et al. [5]	Present Study
De	Ha	d	$f''(0)$	$f''(0)$
0.2	**0.1**	1.2	-1.096254	-1.096250021
0.2	**0.3**	1.2	-1.186286	-1.186284002
0.2	**0.5**	1.2	-1.278458	-1.278455964
0.2	0.2	1.2	-1.141036	-1.141031814
0.5	0.2	1.2	-1.214434	-1.214429330
1.0	0.2	1.2	-1.328572	-1.328565080
0.2	0.2	**1**	-1.152848	-1.152844110
0.2	0.2	**2**	-1.114583	-1.114579720
0.2	0.2	**3**	-1.098555	-1.098554548

International Research Journal of Innovations in Engineering and Technology (IRJIET)

ISSN (online): 2581-3048

Volume 9, Issue 6, pp 42-62, June-2025

https://doi.org/10.47001/IRJIET/2025.906007

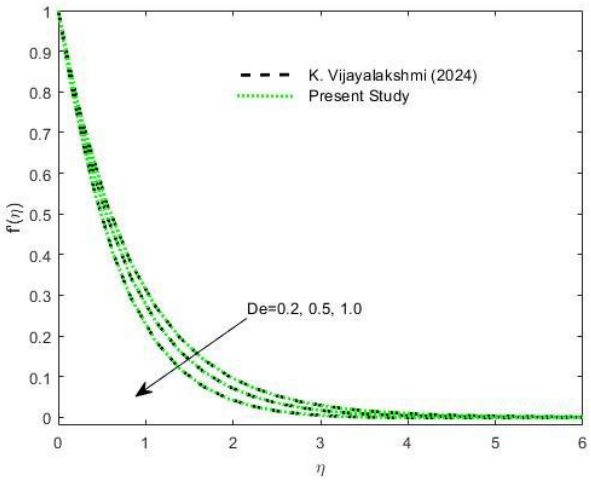

2(a)

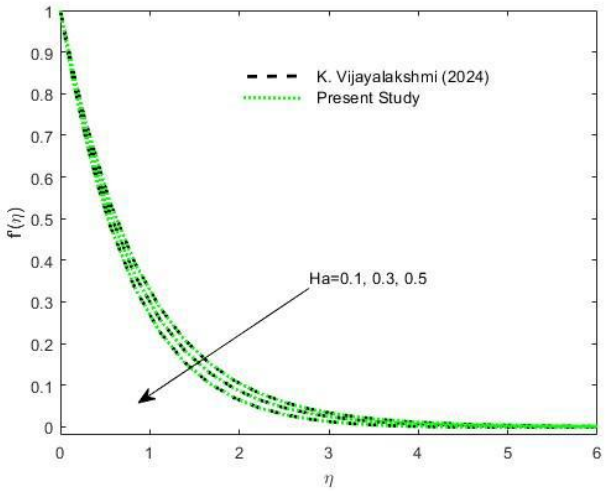

2(b)

Figure 2(a)-(b) shows comparison of velocity profile $f'(\eta)$ for Deborah No. (De) and Hartmann No. (Ha).

Impact of De (Deborah Number):

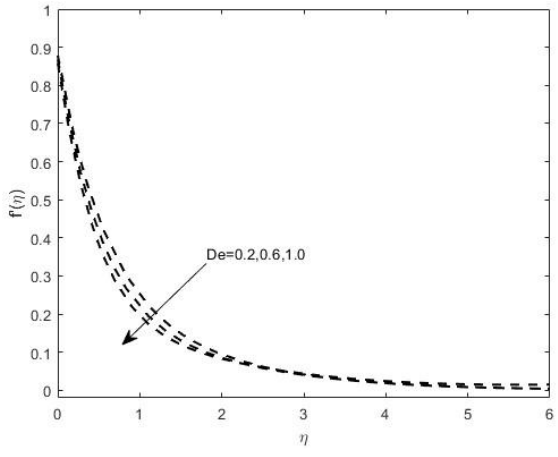

3(a)

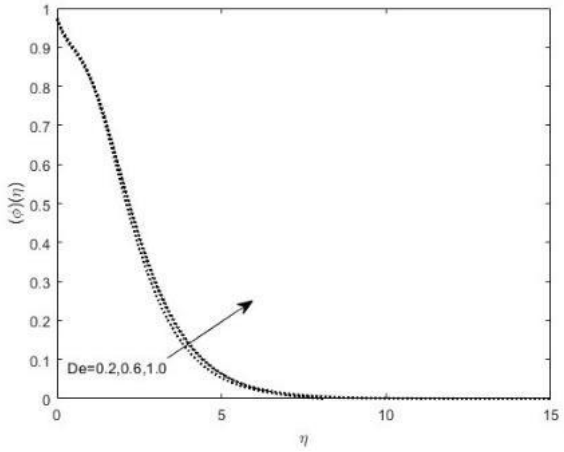

3(b)

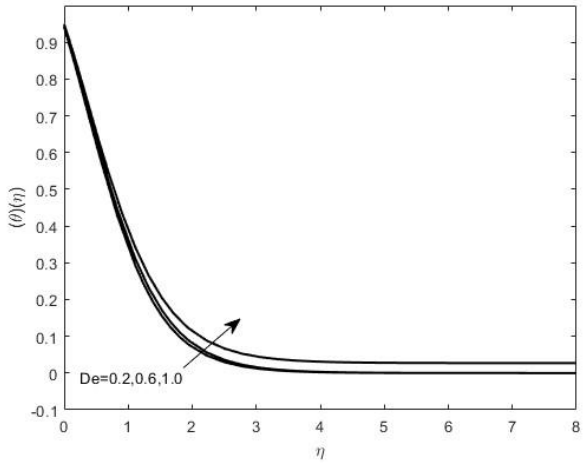

3(c)

Figure 3(a)-3(c) exhibit effect of De (Deborah Number) on velocity, temperature and concentration profiles respectively. The value of other parameter were $K = 1$, $Ha = 0.2$, $d = 1.2$, $Gr = Gc = 0.2$, $Pr = 2$, $Rd = 0.1$, $Nt = Nb = 0.5$, $Ec = 0.2$, $Sc = 0.8$, $\sigma^* = 0.1$, $d_t = 0.5$, $E = 0.1$, $n = 1$, $\lambda_1 = 0.1$, $\lambda_2 = 0.1$, $\lambda_3 = 0.1$ and $s = 0.2$.

Figure3(a)-3(c) illustrate how the velocity, temperature and concentration profile are affected by De.De, that is Deborah number, is a unidimensional property that defines the level of elasticity of a fluid. Increasing De causes a flurry of elasticity-related behavior in the fluid, which causes differentiation in velocity, temperature, and concentrations profile:

Velocity Profile ($De \uparrow \rightarrow$ Velocity $\downarrow$):Increasing De makes the fluid more solid-like in its tendency to refuse deformation, which brings about a decrease in velocity resulting from elastic forces opposing the flow. The thickness of the boundary layer reduces it and confines motion.

Temperature Profile ($De \uparrow \rightarrow$ Temperature $\uparrow$):When measurements of De are high, more internal energy stores are due to elastic effects. This means that the fluid tends to keep more heat, resulting in increased temperature. This indeed

International Research Journal of Innovations in Engineering and Technology (IRJIET)

ISSN (online): 2581-3048

Volume 9, Issue 6, pp 42-62, June-2025

https://doi.org/10.47001/IRJIET/2025.906007

causes the thermal boundary layer to thicken, improving heat transfer.

Concentration Profile ($De \uparrow \rightarrow$ Concentration $\uparrow$):Increased elasticity impacts on mass diffusion so that concentration increases. The concentration boundary layer increases, keeping more solute in it, and thus benefits from this especially when the solvent or solute is polymeric and viscoelastic.

Impression of K(Permeability):

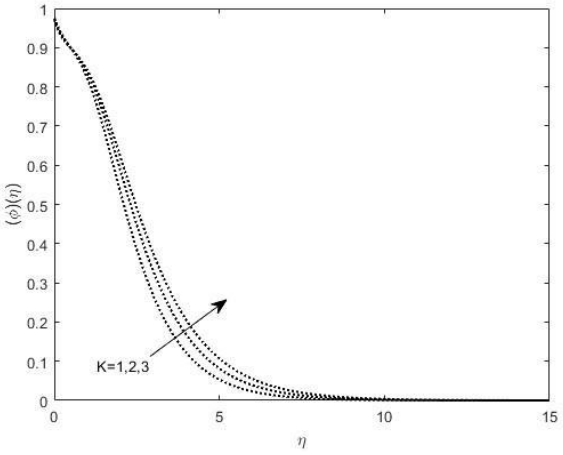

4(a)

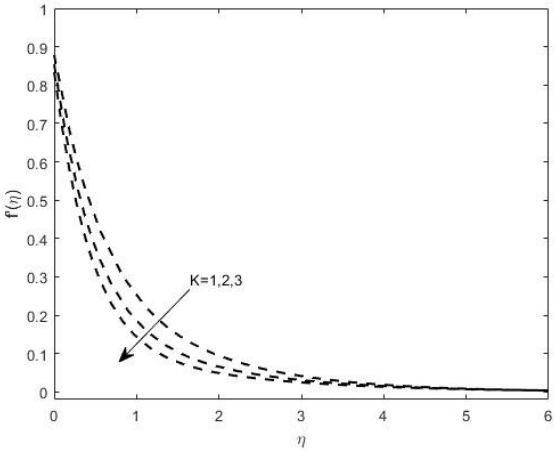

4(b)

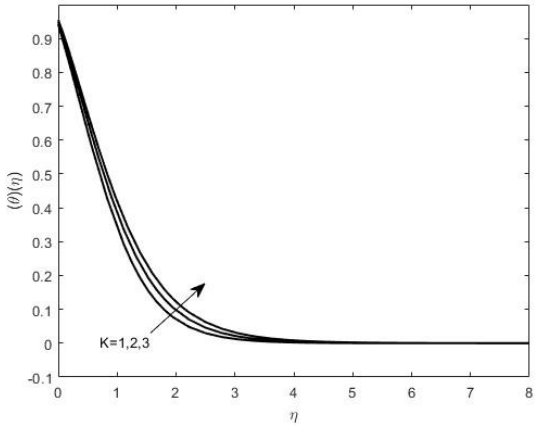

4(c)

Figure 4(a)-4(c) shows effect of K (Permeability) on velocity, temperature and concentration profiles respectively. The value of other parameter were $De = 0.2$, $Ha = 0.2$, $d = 1.2$, $Gr = Gc = 0.2$, $Pr = 2$, $Rd = 0.1$, $Nt = Nb = 0.5$, $Ec = 0.2$, $Sc = 0.8$, $\sigma^* = 0.1$, $d_t = 0.5$, $E = 0.1$, $n = 1$, $\lambda_1 = 0.1$, $\lambda_2 = 0.1$, $\lambda_3 = 0.1$ and $s = 0.2$.

Figure 4(a)-4(c) intimate the effect of permeability (K) on velocity profile, temperature profile and concentration profile. Ever since the incidence of flow pertaining to Maxwell fluids, for which this theory stands, the permeability parameter is vital. An increase in permeability generates a varying effect on the velocity, temperature, and concentration profiles as explained below:

Velocity Profile (Permeability $\uparrow \rightarrow$ Velocity $\downarrow$): With more fluid allowed to pass through the porous medium by increased permeability, resistance to flow increases and velocity thus decreases. The boundary layer thickness decreases, thus inhibiting fluid motion.

Temperature Profile (Permeability $\uparrow \rightarrow$ Temperature $\uparrow$): Increased permeability enhances heat retention within the porous medium, giving a corresponding increase in temperature as the fluid absorbs additional thermal energy. In this case, the thermal boundary layer thickens, improving heat transfer.

Concentration Profile (Permeability $\uparrow \rightarrow$ Concentration $\uparrow$): Higher permeability effectively enhances mass diffusion, hence concentrating more. The concentration boundary layer thickens, allowing enhanced retention by solute. This effect is important in the case of polymeric and viscoelastic fluids in industrial applications.

International Research Journal of Innovations in Engineering and Technology (IRJIET)

ISSN (online): 2581-3048

Volume 9, Issue 6, pp 42-62, June-2025

https://doi.org/10.47001/IRJIET/2025.906007

Influence of Ha (Hartmann Number):

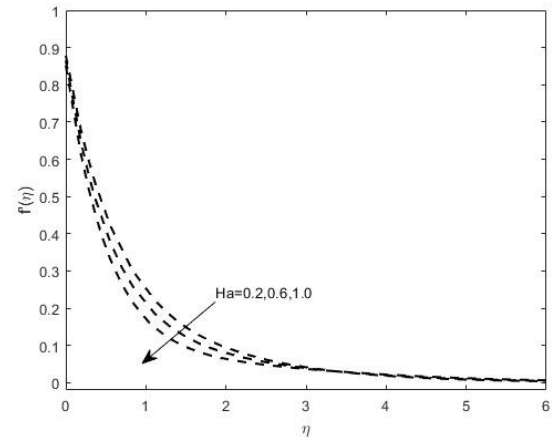

5(a)

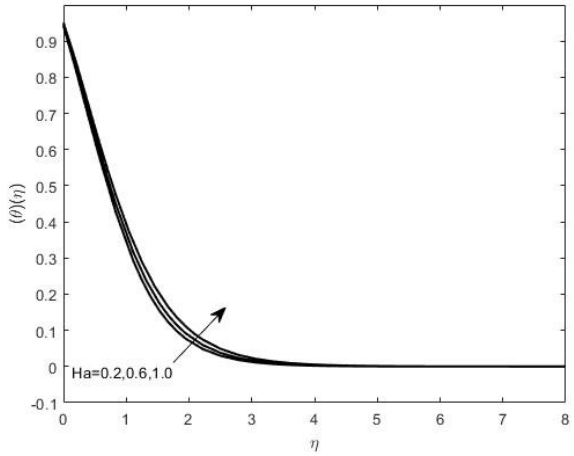

5(b)

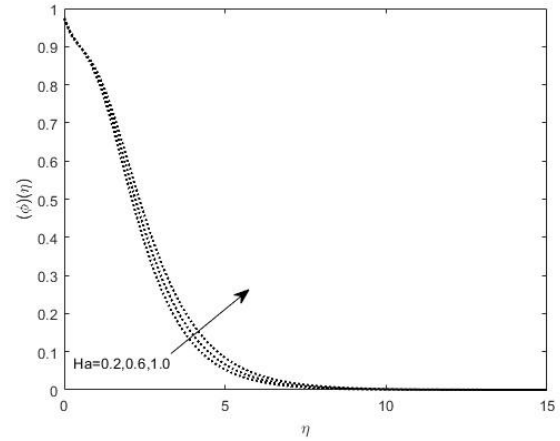

5(c)

Figure 5(a)-5(c) shows effect of Ha (Hartmann No.) on velocity, temperature and concentration profiles respectively. The value of other parameter were $De = 0.2$, $K = 1$, $d = 1.2$, $Gr = Gc = 0.2$, $Pr = 2$, $Rd = 0.1$, $Nt = Nb = 0.5$, $Ec = 0.2$, $Sc = 0.8$, $\sigma^* = 0.1$, $d_t = 0.5$, $E = 0.1$, $n = 1$, $\lambda_1 = 0.1$, $\lambda_2 = 0.1$, $\lambda_3 = 0.1$ and $s = 0.2$.

The Hartmann number is denoted as Ha, which actually indicates the impact of any magnetic field of a conducting fluid. The increasing values of Ha intensify the Lorentz forces acting on the fluid and lead to the following different effects on velocity, temperature, and concentration profiles:

Velocity Profile (Ha ↑→ Velocity ↓): A higher Ha strengthens the magnetic field, increasing the resistance to movement of the fluid. The Lorentz force acts as a drag force, reducing velocity. The boundary layer thickness decreases, restricting fluid motion.

Temperature Profile (Ha ↑→ Temperature ↑): The magnetic field adds to the generation of heat due to Joule heating effects. The result is a higher temperature, since the fluid absorbs more thermal energy. Thus, this greatly thickens the thermal boundary layer, creating a more efficient heat transfer.

Concentration Profile (Ha ↑→ Concentration ↑): Increasing Ha, the mass diffusion increased concentration. The concentration boundary layer expands and thus retains more solute. This effect is most significant in magnetohydrodynamic (MHD) flows, especially in industrial and biomedical applications.

Efficacy of d (Electrode's Width and the magnets):

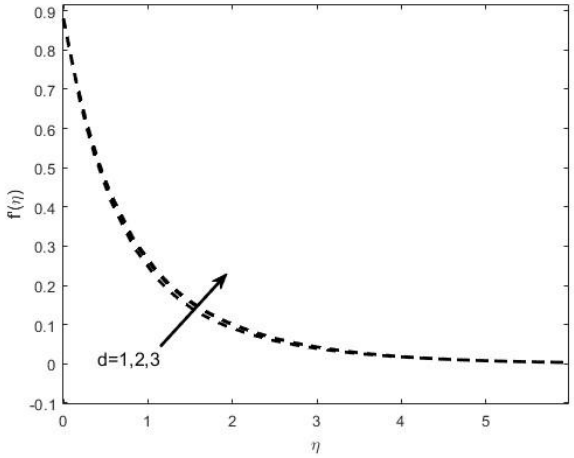

6(a)

Figure 6(a) shows effect of d on velocity profile. The value of other parameter were $De = 0.2$, $K = 1$, $Ha = 0.2$, $Gr = Gc = 0.2$, $Pr = 2$, $Rd = 0.1$, $Nt = Nb = 0.5$, $Ec = 0.2$, $Sc = 0.8$, $\sigma^* = 0.1$, $d_t = 0.5$, $E = 0.1$, $n = 1$, $\lambda_1 = 0.1$, $\lambda_2 = 0.1$, $\lambda_3 = 0.1$ and $s = 0.2$.

The width of the electrodes and the magnetic field strength (d) are critical parameters that affect the motion of a Maxwell fluid, a generic viscoelastic fluid model. As they are increased, they influence the velocity profile in this way:

Velocity Profile (Electrode Width & Magnetic Field ↑→ Velocity ↑)**:** A greater electrode width enhances the electric field, thereby increasing the driving force acting upon the

International Research Journal of Innovations in Engineering and Technology (IRJIET)

ISSN (online): 2581-3048

Volume 9, Issue 6, pp 42-62, June-2025

https://doi.org/10.47001/IRJIET/2025.906007

fluid. Stronger magnetic effects may cause an increase in the electro-magnetohydrodynamic (EMHD) flow, thereby propelling the fluid faster. This general increase in velocity occurs when more forceful propulsion is applied to the fluid.

Dominance of Gr&Gc (Thermal & Mass Grashof Number):

The Thermal Grashof Number (Gr) and Mass Grashof Number (Gc) characterize the buoyancy forces arising from temperature and concentration differences, respectively. Increasing Gr and Gc affects velocity, temperature, and concentration profiles in the following ways:

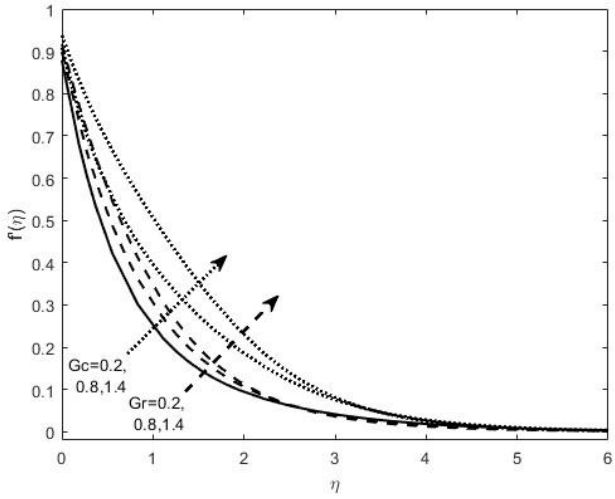

7(a)

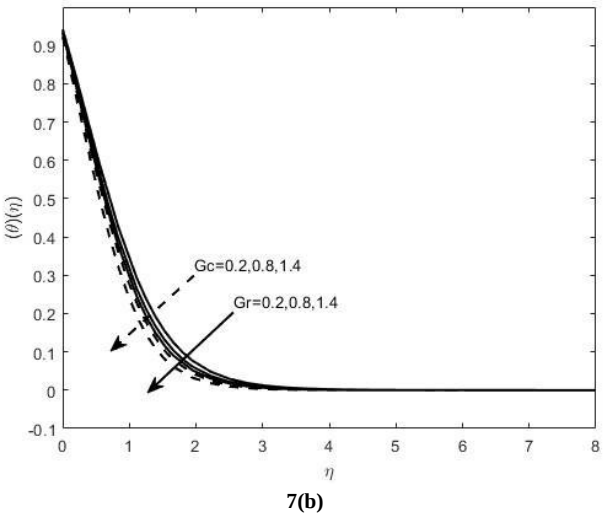

7(b)

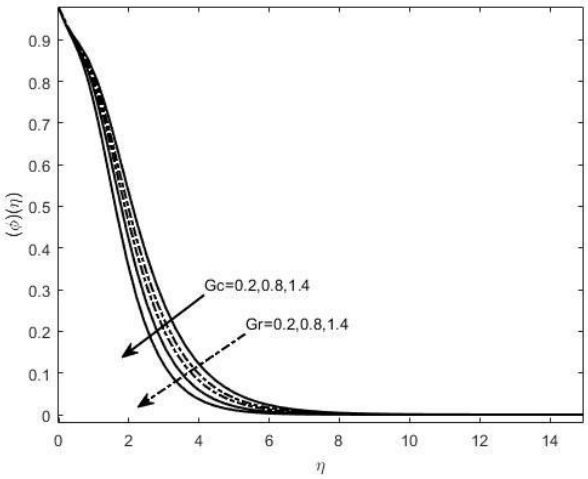

7(c)

Figure 7(a)-7(c) shows impression of Gr&Gc on velocity, temperature and concentration profiles respectively. The value of other parameter were $De = 0.2$, $K = 1$, $Ha = 0.2$, $d = 1.2$, $Pr = 2$, $Rd = 0.1$, $Nt = Nb = 0.5$, $Ec = 0.2$, $Sc = 0.8$, $\sigma^* = 0.1$, $d_t = 0.5$, $E = 0.1$, $n = 1$, $\lambda_1 = 0.1$, $\lambda_2 = 0.1$, $\lambda_3 = 0.1$ and $s = 0.2$.

Velocity Profile ($Gr \uparrow$&$Gc \uparrow \rightarrow$ Velocity $\uparrow$): Higher Gr and Gc facilitate convection, strengthening buoyancy forces and enhancing the upward motion of the fluid. Hence, there is higher velocity, which includes convection effect and wide expansion of the boundary layer, facilitating faster motion of the fluid.

Temperature Profile ($Gr \uparrow$&$Gc \uparrow \rightarrow$ Temperature $\downarrow$): Increased buoyant force promotes heat dissipation, thereby reducing temperature. The thermal boundary layer becomes thinner, further preventing heat buildup. Thus, the fluid experiences enhanced cooling because of a greater convection effect.

Concentration Profile ($Gr \uparrow$&$Gc \uparrow \rightarrow$ Concentration $\downarrow$): The mass transfer is enhanced for more considerable Gc, reducing solute accumulation. So, the shrinking of the concentration boundary layer lowers the concentration profile. This comes into play in natural convection flows, more so in industrial and environmental concern.

Influence of Pr (Prandtl Number):

Prandtl number (Pr) expresses a ratio of momentum diffusivity to thermal diffusivity in the fluid. When an increase in Pr occurs in Maximillian fluid, it will influence the temperature, and concentration profiles in the following way:

International Research Journal of Innovations in Engineering and Technology (IRJIET)

ISSN (online): 2581-3048

Volume 9, Issue 6, pp 42-62, June-2025

https://doi.org/10.47001/IRJIET/2025.906007

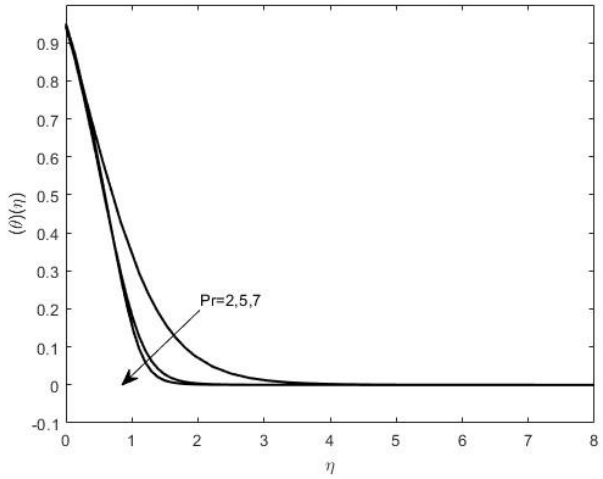

8(a)

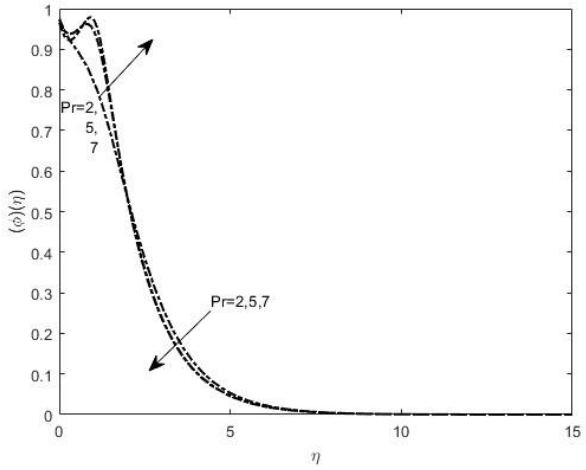

8(b)

Figure 8(a)-8(b) shows impression of Pron temperature and concentration profiles respectively. The value of other parameter were $De = 0.2, K = 1, Ha = 0.2, d = 1.2, Gr = Gc = 0.2, Rd = 0.1, Nt = Nb = 0.5, Ec = 0.2, Sc = 0.8, \sigma^* = 0.1, d_t = 0.5, E = 0.1, n = 1, \lambda_1 = 0.1, \lambda_2 = 0.1, \lambda_3 = 0.1$ and $s = 0.2$.

Temperature Profile ($Pr \uparrow \rightarrow$ Temperature $\downarrow$): Higher Pr means lower thermal conductivity and so slows down the transfer of heat, resulting in a decrease of temperature since less heat is diffusing to the system. The thin thermal boundary layer, in turn, leads to reduced heat accumulation.

Concentration Profile: $Pr \uparrow \rightarrow$ initial increase($\uparrow$), then sudden drop($\downarrow$): A little higher Pr initially enhances mass diffusion, hence triggering an increase in concentration. However, beyond a certain point, when the thermal effect overrides, the concentration boundary layer shrinks and the concentration drop abruptly. This sort of behavior is crucial in polymeric solutions, biomedical fluids, and industrial applications.

Efficacy of Rd (Radiation Parameter):

Radiation Parameter, an important property with significant application in thermal behavior for Maxwell fluids, a viscoelastic fluid model. With the increase in Rd, the following alterations are made to velocity, temperature, and concentration:

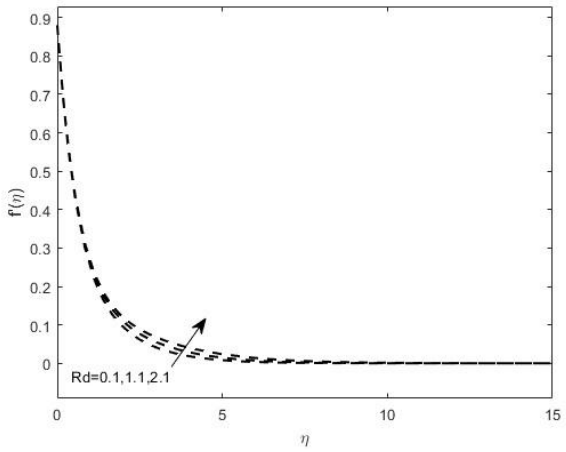

9(a)

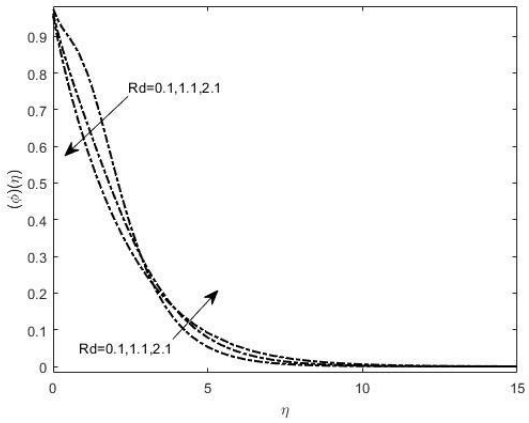

9(b)

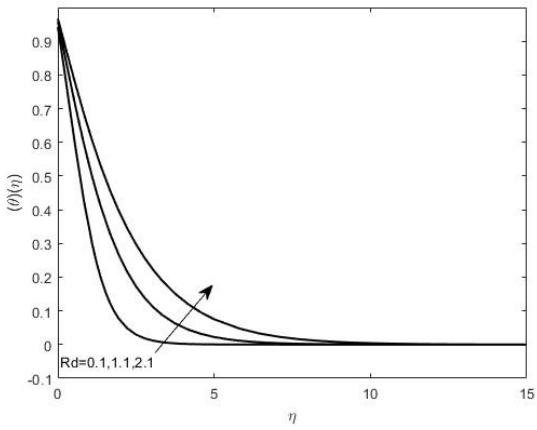

9(c)

Figure 9(a)-9(c) shows impression of Rd on velocity, temperature and concentration profiles respectively. The value of other parameter were $De = 0.2, K = 1, Ha = 0.2, d = 1.2, Gr = Gc = 0.2, Pr = 2, Nt =$

International Research Journal of Innovations in Engineering and Technology (IRJIET)

ISSN (online): 2581-3048

Volume 9, Issue 6, pp 42-62, June-2025

https://doi.org/10.47001/IRJIET/2025.906007

$Nb = 0.5, Ec = 0.2, Sc = 0.8, \sigma^* = 0.1, d_t = 0.5, E = 0.1, n = 1, \lambda_1 = 0.1, \lambda_2 = 0.1, \lambda_3 = 0.1$ and $s = 0.2$.

Velocity Profile ($Rd \uparrow \rightarrow$ Velocity $\uparrow$): The heat transfer enhances the flow velocity with rising Rd, and lowering fluid viscosity as consequence of increased rates of heat transfer through radiation. The fluid moves faster, having lesser resistances offer to the passage of liquid to the wall, and brings about widen-area of boundary layer planes along which fluid travels faster.

Temperature Profile ($Rd \uparrow \rightarrow$ Temperature $\uparrow$): When radiation effects are increased, more thermal energy is absorbed, resulting in the fluid retaining more heat while rising the temperature. The thermal boundary layer improves its efficiency in heat transfer, thickening.

Concentration Profile ($Rd \uparrow \rightarrow$ Initial Decrease$\downarrow$, Then Sudden Increase$\uparrow$): Initially, higher Rd improves mass diffusion and results in temporary decreased concentration. However, once thermal effects dominate that concentration boundary layer, it will be expanded, causing concentration to increase sharply. Such characteristic is interesting in polymeric solutions, biomedical fluids, and industrial applications.

Cinch of Nt (thermophoresis parameter) Nb (brownian motion parameter):

The thermophoresis parameter (Nt) and Brownian motion parameter (Nb) play crucial roles in the behavior of Maxwell fluid, particularly in nanofluid dynamics. Their effects on velocity, temperature, and concentration profiles are as follows:

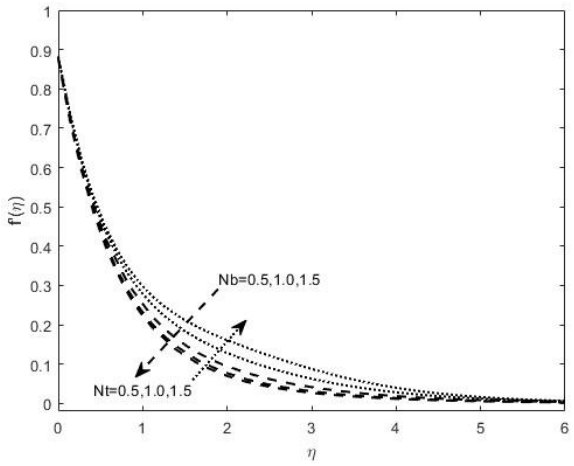

10(a)

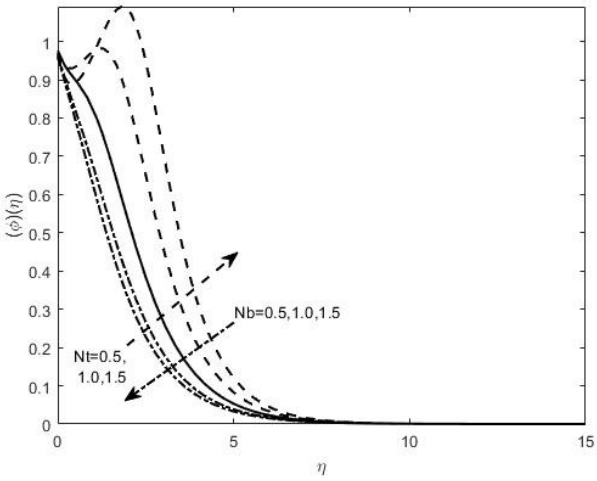

10(b)

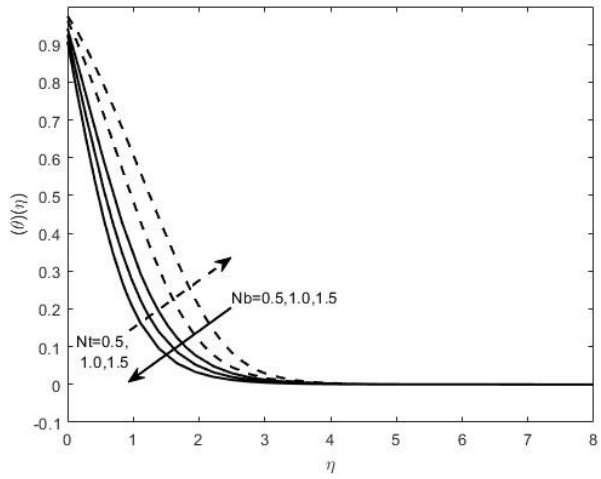

10(c)

Figure 10(a)-10(c) shows impact of Nt & Nb on velocity, temperature and concentration profiles respectively. The value of other parameter were $De = 0.2, K = 1, Ha = 0.2, d = 1.2, Gr = Gc = 0.2, Pr = 2, Rd = 0.1, Ec = 0.2, Sc = 0.8, \sigma^* = 0.1, d_t = 0.5, E = 0.1, n = 1, \lambda_1 = 0.1, \lambda_2 = 0.1, \lambda_3 = 0.1$ and $s = 0.2$.

Velocity profile ($Nt \uparrow \rightarrow$ velocity $\uparrow$): Thermophoresis induces the movement of nanoparticles toward colder regions, thereby increasing the fluid movement that generates a higher velocity profile. The boundary layer will spread to allow for faster movement of fluids.

Temperature profile ($Nt \uparrow \rightarrow$ Temperature $\uparrow$): Thermophoresis enables heat transfer by directing particles away from hotter regions. This results in higher temperatures, where heat is spread much better than before. The thermal boundary layer is thicker, maintaining heat better.

Concentration Profile ($Nt \uparrow \rightarrow$ Concentration $\uparrow$): Nanoparticles move due to temperature gradients which lead

International Research Journal of Innovations in Engineering and Technology (IRJIET)

ISSN (online): 2581-3048

Volume 9, Issue 6, pp 42-62, June-2025

https://doi.org/10.47001/IRJIET/2025.906007

to increased local concentration. Thus, a higher concentration profile suffices as it gathers more particles. The concentration boundary layer grows, benefiting mass transfer.

Velocity Profile ($Nb \uparrow \rightarrow$ Velocity $\downarrow$): Brownian motion causes the erratic motion of nanoparticles to increase fluid resistance. The velocity thus decreases because this random motion disrupts uniformity of flow. The boundary layer becomes thinner, reducing the movement of fluids.

Temperature Profile ($Nb \uparrow \rightarrow$ Temperature $\downarrow$): Brownian motion induces thermal diffusion, allowing for heat dissipation. Therefore, the temperature profile decreases, with heat being dissipated more uniformly. This reduces the thickness of the thermal boundary layer, thereby reducing the accumulation of heat.

Concentration Profile ($Nb \uparrow \rightarrow$ Concentration $\downarrow$): The hectic motion of nanoparticles causes their dispersion, thus reducing the local concentration. The concentration boundary layer becomes thinner, producing a lower concentration profile. This has great significance in polymer solutions, biomedical flows, and industrial applications.

Sway of Sc (Schmidt number):

The Schmidt number (Sc) signifies the ratio of momentum to mass diffusivity of a fluid. In Maxwell fluids, an increased Sc affects the concentration profiles as follow:

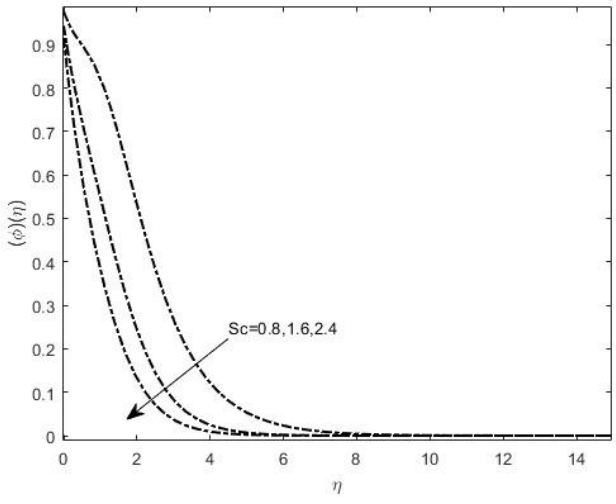

11(a)

Figure 11(a) shows effect of Sc on concentration profile. The value of other parameter were $De = 0.2$, $K = 1$, $Ha = 0.2$, $d = 1.2$, $Gr = Gc = 0.2$, $Pr = 2$, $Rd = 0.1$, $Nt = Nb = 0.5$, $Ec = 0.2$, $\sigma^* = 0.1$, $d_t = 0.5$, $E = 0.1$, $n = 1$, $\lambda_1 = 0.1$, $\lambda_2 = 0.1$, $\lambda_3 = 0.1$ and $s = 0.2$.

Concentration Profile ($Sc \uparrow \rightarrow$ Concentration $\downarrow$): Higher Sc means lower mass diffusivity, which curtails solute transportation. With a reduction in the thickness of the concentration boundary layer, the concentration profile reduces.

Repercussion of σ^*/H (Chemical reaction parameter):

Chemical reactants and fluid mechanics have two important applications in the injection of drug formulation at a Maxwell fluid. So, the "σ^*" parameter seems interesting concerning the application, especially in reactive flows. Here are some effects on it by an increase in σ^* that have been observed:

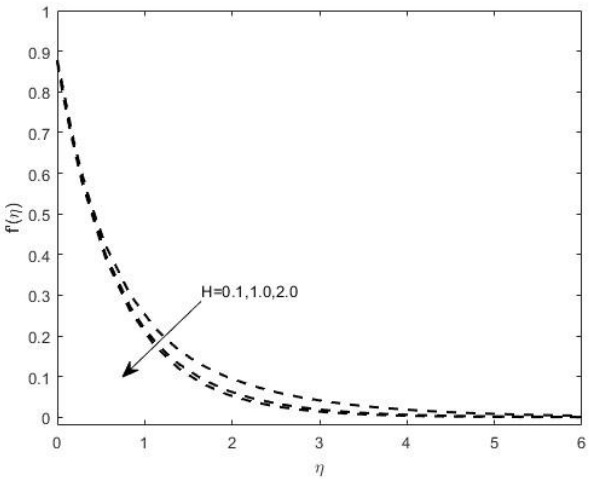

12(a)

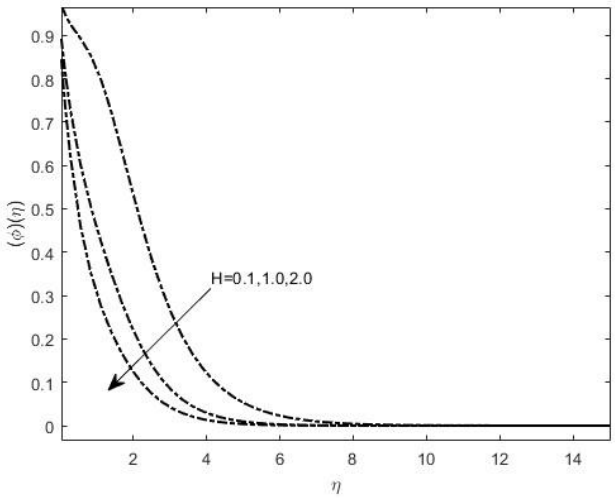

12(b)

International Research Journal of Innovations in Engineering and Technology (IRJIET)

ISSN (online): 2581-3048

Volume 9, Issue 6, pp 42-62, June-2025

https://doi.org/10.47001/IRJIET/2025.906007

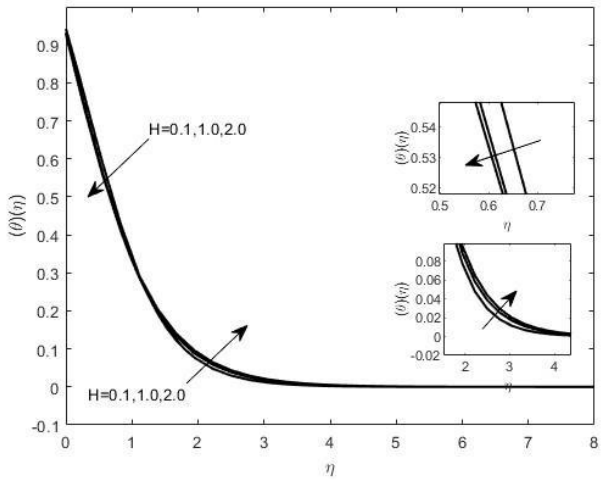

12(c)

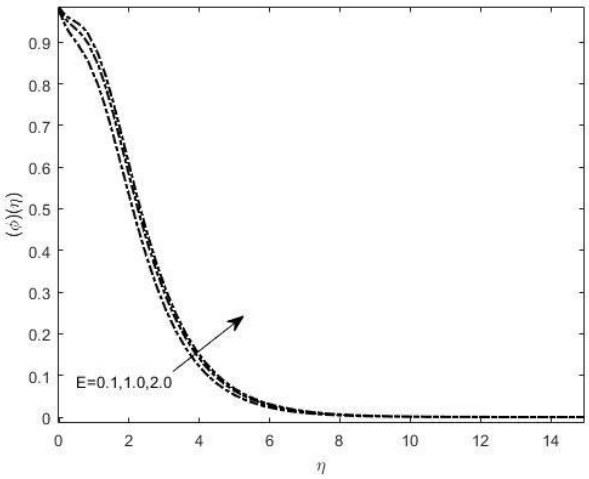

13(a)

Figure 12(a)-12(c) shows impact of H/σ^* on velocity, temperature and concentration profiles respectively. The value of other parameter were $De = 0.2$, $K = 1$, $Ha = 0.2$, $d = 1.2$, $Gr = Gc = 0.2$, $Pr = 2$, $Rd = 0.1$, $Nt = Nb = 0.5$, $Ec = 0.2$, $Sc = 0.8$, $d_t = 0.5$, $E = 0.1$, $n = 1$, $\lambda_1 = 0.1$, $\lambda_2 = 0.1$, $\lambda_3 = 0.1$ and $s = 0.2$.

Figure 13(a) shows efficacy of E on concentration profile. The value of other parameter were $De = 0.2$, $K = 1$, $Ha = 0.2$, $d = 1.2$, $Gr = Gc = 0.2$, $Pr = 2$, $Rd = 0.1$, $Nt = Nb = 0.5$, $Ec = 0.2$, $Sc = 0.8$, $\sigma^* = 0.1$, $d_t = 0.5$, $n = 1$, $\lambda_1 = 0.1$, $\lambda_2 = 0.1$, $\lambda_3 = 0.1$ and $s = 0.2$.

Velocity profile ($\sigma^* \uparrow \rightarrow$ Velocity$\downarrow$): It increases the reaction kinetics for chemical reactions and increases fluid resistance. More reactive species get consumed, thereby restricting the movement of the fluid through the velocity profile. It leads to a decrease in velocity profile and shocked boundary layer thickness.

Temperature profile ($\sigma^* \uparrow \rightarrow$ decrease first$\downarrow$, then a sudden increase$\uparrow$) : Higher σ^* initially leads to heat absorption (because of endothermic reaction) which makes the temperature drop. Exothermic effects become more pronounced as the reaction progresses, suddenly increasing temperature. Thermal boundary layer increased and heat transfer efficiencies improved.

Concentration profile ($\sigma^* \uparrow \rightarrow$ Concentration $\downarrow$): Increasing σ^* raises reactant consumption and, therefore, decreases reactant concentration. Alike, the concentration boundary layer shrinks resulting in a decrease in concentration profile.

Influence of E (Activation Energy):

Activation energy (E) becomes an important characteristic in the flow behavior of Maxwell fluid especially in the chemically reactive flows. An increase in E influences the profile concentration in the following manner:

Concentration profile: ($E \uparrow \rightarrow$ Concentration $\uparrow$): With an increase in E, the reactant is consumed at a lower rate which allows more particles to remain in the fluid, thus increasing the concentration. The decrease in the transformation of molecules leads to the expansion of the concentration boundary layer resulting in a good retention of mass.

Dominance of s (Suction/Injection coefficient):

The parameter for suction/injection (s) prominently influences the behavior of Maxwell fluids with regard to boundary layer control. An increase in s brings the following behavior alterations in the velocity, temperature, and concentration profiles:

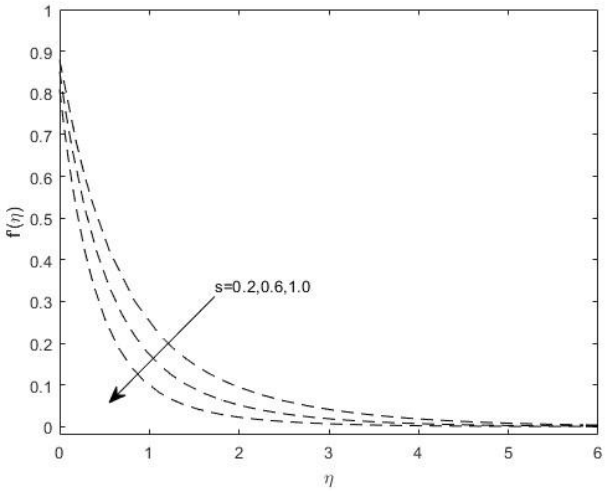

14(a)

International Research Journal of Innovations in Engineering and Technology (IRJIET)

ISSN (online): 2581-3048

Volume 9, Issue 6, pp 42-62, June-2025

https://doi.org/10.47001/IRJIET/2025.906007

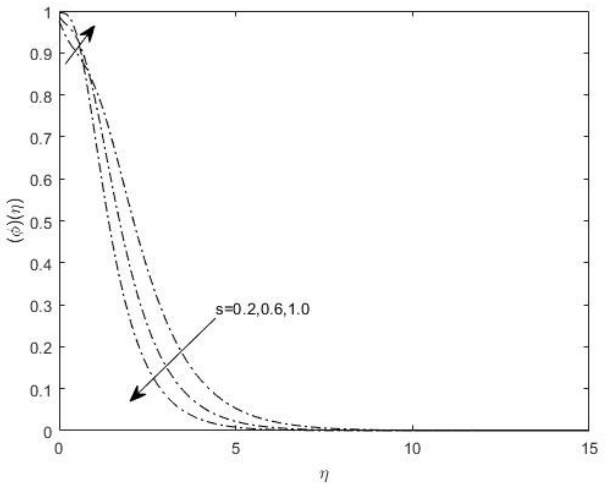

14(b)

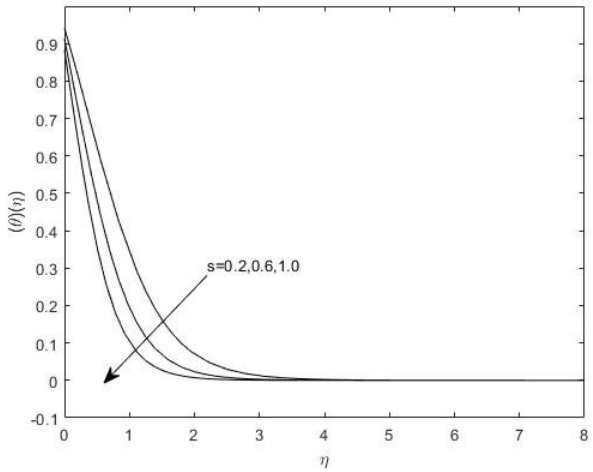

14(c)

Figure 14(a)-14(c) shows efficacy of s on velocity, temperature and concentration profiles respectively. The value of other parameter were $De = 0.2, K = 1, Ha = 0.2, d = 1.2, Gr = Gc = 0.2, Pr = 2, Rd = 0.1, Nt = Nb = 0.5, Ec = 0.2, Sc = 0.8, \sigma^* = 0.1, d_t = 0.5, n = 1, \lambda_1 = 0.1, \lambda_2 = 0.1, \lambda_3 = 0.1$ and $E = 0.1$.

The parameter for suction/injection (s) prominently influences the behavior of Maxwell fluids with regard to boundary layer control. An increase in s brings the following behavior alterations in the velocity, temperature, and concentration profiles:

Velocity Profile ($s \uparrow \rightarrow$ Velocity $\downarrow$): Suction extracts fluid from the boundary layer, transferring momentum away and retarding the flow. This consequently drives down the velocity since resistance offered to the fluid increases. The thickness of the boundary layer decreases, hampering fluid movement.

Temperature profile ($s \uparrow \rightarrow$ Temperature $\downarrow$): Suction augments dissipation of heat, thus diminishing retention of thermal energy. Hence the temperature profile declines, heat being withdrawn more efficiently. The thermal boundary layer is squished, hampering accumulation of heat.

Concentration Profile ($s \uparrow \rightarrow$ Initial Increase $\uparrow$, Then Sudden Decrease $\downarrow$): Initially, suction aids in mass transport, thus temporarily increasing concentration. However, as removal of fluid continues, the concentration boundary layer undergoes shrinkage and concentration plunges abruptly.

Effect of λ_1, λ_2, λ_3 (Velocity Slip, Thermal Slip and Concentration Slip):

The slip parameters (λ_1, λ_2, λ_3) are the most important criteria to investigate behavior of Maxwell fluid, especially in boundary layer dynamics. Their effects are different on velocity, temperature, and concentration profiles as discussed below:

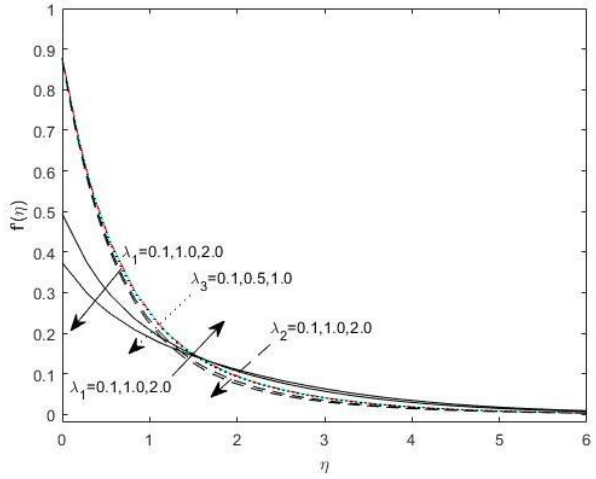

15(a)

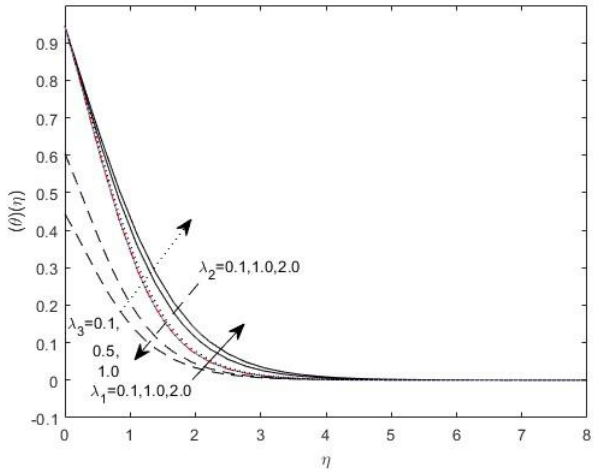

15(b)

International Research Journal of Innovations in Engineering and Technology (IRJIET)

ISSN (online): 2581-3048

Volume 9, Issue 6, pp 42-62, June-2025

https://doi.org/10.47001/IRJIET/2025.906007

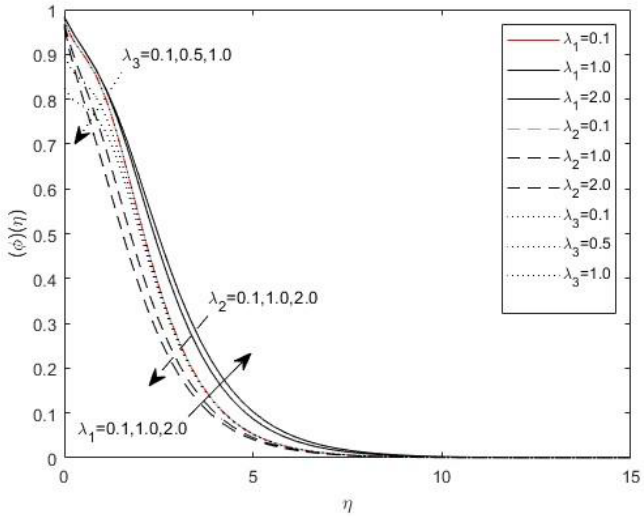

15(c)

Figure 15(a)-15(c) shows efficacy of λ_1, λ_2, λ_3 on velocity, temperature and concentration profiles respectively. The value of other parameter were $De = 0.2$, $K = 1$, $Ha = 0.2$, $d = 1.2$, $Gr = Gc = 0.2$, $Pr = 2$, $Rd = 0.1$, $Nt = Nb = 0.5$, $Ec = 0.2$, $Sc = 0.8$, $\sigma^* = 0.1$, $d_t = 0.5$, $n = 1$, $s = 0.2$ and $E = 0.1$.

A. Effect of Increasing Velocity Slip (λ_1):

Velocity Profile ($\lambda_1 \uparrow \rightarrow$ Initial Decrease↑, Then Sudden Increase↓): Initially, velocity slip causes a reduction in momentum transfer, hence a decrease in velocity. However, when the slip effects dominate, the fluid would experience enhanced motion leading to a sudden increase in velocity. The boundary layer adjusts dynamically based on the intensity of slip.

Temperature Profile ($\lambda_1 \uparrow \rightarrow$ Temperature ↑): Increasing the velocity slip improves the movement of the fluid and hence enhances heat transfer, resulting in temperatures that are higher than before because of better conducted energy distribution involving thermal energy. In fact, the thermal boundary layer thickens, retaining heat more.

Concentration Profile ($\lambda_1 \uparrow \rightarrow$ Concentration ↑): More slip means enhanced transport of mass and therefore can attain higher concentration. The concentration boundary layer expands and allows more solute accumulation. It holds much importance in polymeric solutions and biomedical applications.

B. Effect of Increasing Thermal Slip (λ_2):

Velocity Profile ($\lambda_2 \uparrow \rightarrow$ Velocity ↓): Thermal slip reduces the efficiency of heat transfer to the fluid, thereby increasing resistance to flow and causing a decrease in velocity, with thermal contributions weakening motion in the fluid. The boundary layer thickness reduces, restricting fluid movement.

Temperature Profile ($\lambda_2 \uparrow \rightarrow$ Lower Temperature↓): Due to thermal slip, conduction of heat becomes limited, which decreases temperature. Consequently, it has a lower temperature profile because diffusion of heat is less efficient. Therefore, the thermal boundary layer shrinks, resulting in lower amounts of heat retained.

Concentration Profile ($\lambda_2 \uparrow \rightarrow$ Concentration ↓): Lower thermal effects decrease the effectiveness of mass diffusion, thereby dropping concentration. Consequently, there would be a decreased concentration profile because of the concentrated boundary layer that forms. This phenomenon can be noted in chemical processing and environmental engineering.

C. Effect of Increasing Concentration Slip (λ_3):

Velocity Profile ($\lambda_3 \uparrow \rightarrow$ Velocity ↓): The impact of concentration slip on mass transfer is that it was reduced along with an accompanying increase in fluid resistance. Thus, the velocity drops since the solute effect weakened fluid movement. The boundary layer thickness reduces, restricting fluid movement.

Temperature Profile ($\lambda_3 \uparrow \rightarrow$ Temperature ↑): Concentration slip has effects on changing the thermal diffusion, leading to higher temperature. The thermal boundary layer thickens, improving heat retention. This effect is significant in polymeric solutions and biomedical applications.

Concentration Profile ($\lambda_3 \uparrow \rightarrow$ Concentration ↓): Increase in slip, hence weakened solute retention, decreases concentration. The concentration boundary layer shrinks, leading to a lower concentration profile. This behavior is commonly observed in chemical processing and advanced cooling systems.

International Research Journal of Innovations in Engineering and Technology (IRJIET)

ISSN (online): 2581-3048

Volume 9, Issue 6, pp 42-62, June-2025

https://doi.org/10.47001/IRJIET/2025.906007

Table 2: Indicate effect of various parameters on $f''(0)$,$\theta'(0)$,$\phi'(0)$while other parameter remains constant $De = 0.2$, $K = 1$, $Ha = 0.2$, $d = 1.2$, $Gr = Gc = 0.2$, $Pr = 2$, $Rd = 0.1$, $Nt = Nb = 0.5$, $Ec = 0.2$, $Sc = 0.8$, $\sigma^* = H = 0.1$, $d_t = dt = 0.5$, $E = 0.1$, $n = 1$, $\lambda_1 = l1 = 0.1$, $\lambda_2 = l2 = 0.1$, $\lambda_3 = l3 = 0.1$ and $s = 0.2$.

De	K	Ha	Gr	Gc	Rd	Nb	Nt	Sc	E	s	$f''(0)$	$\theta'(0)$	$\phi'(0)$
0.2	1	0.2	0.2	0.2	0.1	0.5	0.5	0.8	0.1	0.2	-1.214602668	0.656750221	0.243991084
0.6	1	0.2	0.2	0.2	0.1	0.5	0.5	0.8	0.1	0.2	-1.317947268	0.619577253	0.253548021
1.0	1	0.2	0.2	0.2	0.1	0.5	0.5	0.8	0.1	0.2	-1.420876101	0.583115407	0.272677824
0.2	**2**	0.2	0.2	0.2	0.1	0.5	0.5	0.8	0.1	0.2	-1.462302700	0.572810354	0.263937603
0.2	**3**	0.2	0.2	0.2	0.1	0.5	0.5	0.8	0.1	0.2	-1.660623032	0.507316208	0.284965780
0.2	1	**0.6**	0.2	0.2	0.1	0.5	0.5	0.8	0.1	0.2	-1.347913092	0.610232697	0.255056435
0.2	1	**1.0**	0.2	0.2	0.1	0.5	0.5	0.8	0.1	0.2	-1.483082652	0.558214653	0.269448100
0.2	1	0.2	**0.8**	0.2	0.1	0.5	0.5	0.8	0.1	0.2	-1.015088981	0.716897199	0.230199110
0.2	1	0.2	**1.4**	0.2	0.1	0.5	0.5	0.8	0.1	0.2	-0.829764632	0.763056084	0.221471225
0.2	1	0.2	0.2	**0.8**	0.1	0.5	0.5	0.8	0.1	0.2	-0.904819881	0.784857323	0.235566798
0.2	1	0.2	0.2	**1.4**	0.1	0.5	0.5	0.8	0.1	0.2	-0.625033198	0.864329040	0.233159000
0.2	1	0.2	0.2	0.2	**1.1**	0.5	0.5	0.8	0.1	0.2	-1.207198036	1.064554007	0.361901581
0.2	1	0.2	0.2	0.2	**2.1**	0.5	0.5	0.8	0.1	0.2	-1.202428561	1.284154277	0.437470516
0.2	1	0.2	0.2	0.2	0.1	**1.0**	0.5	0.8	0.1	0.2	-1.235993017	0.845172697	0.337529638
0.2	1	0.2	0.2	0.2	0.1	**1.5**	0.5	0.8	0.1	0.2	-1.247866006	1.052255040	0.361852864
0.2	1	0.2	0.2	0.2	0.1	0.5	**1.0**	0.8	0.1	0.2	-1.185894126	0.412151644	0.281331817
0.2	1	0.2	0.2	0.2	0.1	0.5	**1.5**	0.8	0.1	0.2	-1.170206776	0.279675201	0.412152311
0.2	1	0.2	0.2	0.2	0.1	0.5	0.5	**1.6**	0.1	0.2	-1.245438341	0.737825279	0.566901177
0.2	1	0.2	0.2	0.2	0.1	0.5	0.5	**2.4**	0.1	0.2	-1.262637742	0.788124443	0.833350464
0.2	1	0.2	0.2	0.2	0.1	0.5	0.5	0.8	**1.0**	0.2	-1.209347278	0.643403882	0.184077914
0.2	1	0.2	0.2	0.2	0.1	0.5	0.5	0.8	**2.0**	0.2	-1.206575785	0.636406076	0.151291486
0.2	1	0.2	0.2	0.2	0.1	0.5	0.5	0.8	0.1	**0.6**	-1.498078576	0.986616916	0.131224343
0.2	1	0.2	0.2	0.2	0.1	0.5	0.5	0.8	0.1	**1.0**	-1.918372303	1.321677358	0.031729959

V. CONCLUSION

The study presented a comprehensive analysis of the influence of activation energy and chemical reactions on heat and mass transfer in a Maxwell fluid flow over a Riga plate embedded in porous media. The analysis stands to suggest that a thorough understanding of complex relationships linking velocity, temperature, and concentration profiles would significantly expand the border of knowledge in non-Newtonian dynamics.

- **Velocity Profile Conclusion:**
  It was found that activation energy enhances motion, thus increasing the velocity profiles as chemical reactions were reduced and molecular transformations were somewhat delayed. The chemical reaction parameter (σ^*) and temperature difference (d_t) set up counteracting forces, gradually suppressing the velocity because of the effects of reactant depletion on momentum transfer. The slip conditions are thereby complicating the dynamics of the fluid and would lead for non-linear changes in the velocity distribution. The constraints, apart from these, are imposed by magnetic forces (Ha) and permeability effects that act in the furtherance of the retardation mechanism within the porous medium.
- **Temperature Profile Conclusion:**
  Thermal energy dynamics showed complex interactions between heat dissipation and energy absorption mechanisms, where the influence of the activation energy parameter (E) was found to cool down the fluid by reducing the heat generation rate, while the radiation parameter (Rd) and Eckert number (Ec) resulted in

International Research Journal of Innovations in Engineering and Technology (IRJIET)

ISSN (online): 2581-3048

Volume 9, Issue 6, pp 42-62, June-2025

https://doi.org/10.47001/IRJIET/2025.906007

increased temperature due to thermal diffusion and viscous dissipation. Also, the Schmidt number (Sc) and suction parameter (s) jointly reduced heating by restraining molecular movement while thermophoresis (Nt) increased thermal energy by promoting the migration of nanoparticles. The thermal slip condition (λ_2) greatly lowered temperature by reducing conduction efficiency, while the reaction offered a sudden upsurge in accumulating heat, thereby coming in to support reaction kinetics.

- **Concentration Profile Conclusion:**
  The concentration distribution was subject to a two-phase behavior which after an initial reduction, came into concentration recovery due to rapid depletion of reactants fueling the enhancement by molecular diffusion. The chemical reaction parameter (σ^*) and Brownian motion parameter (Nb) caused solute depletion, increasing the inhibition to mass transport. However, thermophoresis (Nt) and activation energy (E) fostered solute accumulation due to changes in nanoparticle motion and reaction kinetics. Slip conditions (λ_3 and velocity slip λ_1) were also key in the amount of concentration adjustment, showing how the boundary layer modifications have effect on molecular diffusion. The above observations tend to confirm the coupling of both heat and mass transfer, indicating that concentration phenomena cannot be divorced from thermal and velocity effects.

VI. NOVELTY OF THIS RESEARCH

This research offers a pioneering viewpoint on the complicated influences of activation energy and chemical reactions on Maxwell fluid behavior, thereby establishing new correlations between electromagnetic interaction, enhancement of heat transfer, and concentration dynamics. The application of Riga plates in porous media adds an unprecedented dimension to fluid mechanics by providing insight into advanced strategies for boundary-layer control. The advent of multiple slip conditions serves as a novel approach for the optimization of both fluid flow and mass transport, making the study a defining one in the design of industrial processes that use non-Newtonian fluids.

VII. FUTURE SCOPE OF THIS RESEARCH

The present findings open avenues for multidimensional studies, which will include:

- Experimental validation of the theoretical results reinforcing practical applicability of Maxwell fluid dynamics in real-world systems.
- Extension unto interactions of nanofluids, taking into account hybrid nanoparticles for assessing their thermal and concentration-enhancing effects.
- Boundary-layer control optimization techniques in aerospace and biomedical engineering applications.
- Dynamics of time-dependent flow models investigating transient effects and dynamic pressure variations.
- Energy system applications such as solar collectors, geothermal reservoirs, and magnetohydrodynamic (MHD) propulsion systems, which are where activation energy is critical to fluid performance.

This study proves a solid foundation for future explorations of non-Newtonian fluid behavior, thereby contributing to advancing scientific knowledge in chemical, environmental, and engineering arenas.

VIII. NOMENCLATURE

u, v = velocity in x and y direction

κ_1 = Permeability of porous media

μ = viscosity

λ = fluid relaxation time

ρ = fluid density

J_0 = applied current density of the electrodes

M_0 = magnetization of the permanent magnets

ν = kinematic viscosity

$De = \lambda c$ (Deborah Number)

$K = \frac{\nu}{\kappa_1 c}$ (Porosity Number)

$Ha = \frac{\pi J_0 M_0}{8\rho c^2 x}$ (Modified Hartmann Number)

$Gr = \frac{g\beta'(T_w - T_\infty)}{c^2 x}$ (Thermal Grashof Number)

$Gc = \frac{g\beta^*(C_w - C_\infty)}{c^2 x}$ (Mass Grashof Number)

$d = \frac{\pi}{a}\sqrt{\frac{\nu}{c}}$ (Electrode's width and the magnets)

κ^* = slip parameter

c_p = specific heat capacity

σ = Stefen-Boltzmann coefficient

k = thermal conductivity

International Research Journal of Innovations in Engineering and Technology (IRJIET)

ISSN (online): 2581-3048

Volume 9, Issue 6, pp 42-62, June-2025

https://doi.org/10.47001/IRJIET/2025.906007

τ = the ratio of nanoparticle heat capacity to the fluid heat capacity

D_B = variable mass diffusivity

D_T = thermophoretic diffusion coefficient

$Pr = \frac{\mu C_p}{\kappa^*}$ (Prandtl Number)

$Rd = \frac{4\sigma T_\infty}{k\kappa^*}$ (Radiation Parameter)

$Nt = \frac{\tau D_T (T_w - T_\infty)}{T_\infty \nu}$ (thermophoresis parameter)

$Nb = \frac{\tau D_B (C_w - C_\infty)}{\nu}$ (brownian motion parameter)

$Ec = \frac{U_w^2}{c_p (T_w - T_\infty)}$(Eckert Number)

$Sc = \frac{\nu}{D_B}$ (Schmidt number)

$\sigma^* = \frac{k_c}{c}$ (Chemical reaction parameter)

$d_t = \frac{T_w - T_\infty}{T_\infty}$ (Temperature difference)

$E = \frac{E_c}{\kappa\, T_\infty}$ (Activation Energy)

$s = \frac{v_w}{\sqrt{b\nu}}$ = (suction/injection coefficient)

u_w = Surface velocity

v_w = Suction velocity

T_w = Melting temperature

T_∞ = Free stream temperature

C_w = Fluid concentration of wall

L_1,L_2,L_3 = Velocity slip,Thermal slip and Concentration slip factors

$\lambda_1 = L_1 \frac{\sqrt{b}}{\sqrt{\nu}}$(Velocity slip parameter)

$\lambda_2 = L_2 \frac{\sqrt{b}}{\sqrt{\nu}}$(thermal slip parameter)

$\lambda_3 = L_2 \frac{\sqrt{b}}{\sqrt{\nu}}$ (concentration slip parameter)

$f'(\eta)$ = Non dimensional velocity parameter

$g(\eta)$ = Non dimensional microrotation parameter

$\theta(\eta)$ = Non dimensional temperature parameter

$\phi(\eta)$ = Non dimensional concentration parameter

REFERENCES

[1] A. Gailitis and O. Lielausis, "On a possibility to reduce the hydrodynamic resistance of a plate in an electrolyte.," *Appl. Magnetohydrodyn*, p. 143–146, 1961.

[2] L. Parasuraman and D. Krishnamurthy, "Heat and mass transfer analysis of casson fluid flow on a permeable riga-plate," *Indian Journal of Pure & Applied Physics (IJPAP)*, vol. 58, no. 2, pp. 79-86, 2020.

[3] A. T. Adeosun, J. A. Gbadeyan and R. S. Lebelo, "Heat transport of Casson nanofluid flow over a melting Riga plate embedded in a porous medium," *International Journal of Engineering Research in Africa*, vol. 55, pp. 15-27, 2021.

[4] R. Sindhu, N. Alessa, S. Eswaramoorthi and K. Loganathan, "Comparative analysis of darcy–forchheimer radiative flow of a water-based Al2O3-Ag/TiO2 hybrid nanofluid over a riga plate with heat sink/source.," *Symmetry*, vol. 15, no. 1, p. 199, 2023.

[5] K. Vijayalakshmi , A. Chandulal, H. Alhazmi, A. F. Aljohani and I. Khan, "Effect of chemical reaction and activation energy on Riga plate embedded in a permeable medium over a Maxwell fluid flow," *Case Studies in Thermal Engineering*, vol. 59, pp. 1-17, 2024.

[6] S. Abdal, I. Siddique, A. Alshomrani, F. Jarad, I. Din and S. Afzal, "Significance of chemical reaction with activation energy for Riga wedge flow of tangent hyperbolic nanofluid in existence of heat source," *Case Studies in Thermal Engineering*, vol. 28, p. 101542, 2021.

[7] S. Khatun, M. Islam, M. Mollah, S. Poddar and M. Alam, "EMHD radiating fluid flow along a vertical Riga plate with suction in a rotating system," *SN Applied Sciences*, vol. 3, pp. 1-14, 2021.

[8] B. Sharma, R. Gandhi, N. Mishra and Q. Al-Mdallal, "Entropy generation minimization of higher-order endothermic/exothermic chemical reaction with activation energy on MHD mixed convective flow over a stretching surface," *Scientific reports*, vol. 12, no. 1, p. 17688, 2022.

ISSN (online): 2581-3048
Volume 9, Issue 6, pp 42-62, June-2025
https://doi.org/10.47001/IRJIET/2025.906007

[9] U. Raju, S. Rangabashyam, H. Alhazmi and I. Khan, "Irreversible and reversible chemical reaction impacts on convective Maxwell fluid flow over a porous media with activation energy," *Case Studies in Thermal Engineering*, vol. 61, p. 104821, 2024.

[10] M. Rafiq, A. Shaheen, Y. Trabelsi, S. Eldin, M. Khan and D. Suker, "mpact of activation energy and variable properties on peristaltic flow through porous wall channel," *Scientific Reports*, vol. 13, no. 1, p. 3219, 2023.

[11] U. Khan, Z. Mahmood, S. Eldin, B. Makhdoum, B. Fadhl and A. Alshehri, "Mathematical analysis of heat and mass transfer on unsteady stagnation point flow of Riga plate with binary chemical reaction and thermal radiation effects," *Heliyon*, vol. 9, no. 3, 2023.

[12] M. Parvine, M. Mollah, S. Poddar, M. Alam and G. Lorenzini, "EMHD Nanofluid Flow Along A Porous Riga Plate With Thermal Radiation," *JOURNAL OF MECHANICAL ENGINEERING RESEARCH AND DEVELOPMENTS*, vol. 44, no. 9, pp. 140-155, 2021.

[13] K. Loganathan, N. Alessa, R. Jain, F. Ali and A. Zaib, "Dynamics of heat and mass transfer: Ree-Eyring nanofluid flow over a Riga plate with bioconvention and thermal radiation.," *Frontiers in Physics*, vol. 10, p. 974562, 2022.

[14] F. Ali, C. Reddy, N. Summayya and M. Ahmed, "Effect of nonlinear thermal radiation on unsteady MHD flow of Maxwell nanoliquid over a porous vertical sheet with chemical reaction," *Heat Transfer*, vol. 50, no. 8, pp. 8259-8279, 2021.

[15] S. Abdal, I. Siddique, D. Alrowaili, Q. Al-Mdallal and S. Hussain, "Exploring the magnetohydrodynamic stretched flow of Williamson Maxwell nanofluid through porous matrix over a permeated sheet with bioconvection and activation energy," *Scientific reports*, vol. 12, no. 1, p. 278, 2022.

[16] B. Ishtiaq, S. Nadeem and N. Abbas, "Theoretical study of two-dimensional unsteady Maxwell fluid flow over a vertical Riga plate under radiation effects," *Scientia Iranica*, vol. 29, no. 6, pp. 3072-3083, 2022.

[17] H. Waqas, M. Oreijah, K. Guedri, S. Khan, S. Yang, S. Yasmin and A. Galal, "Gyrotactic motile microorganisms impact on pseudoplastic nanofluid flow over a moving Riga surface with exponential heat flux," *Crystals*, vol. 12, no. 9, p. 1308, 2022.

[18] S. Li, K. Raghunath, A. Alfaleh, F. Ali, A. Zaib, M. Khan, S. ElDin and V. Puneeth, "Effects of activation energy and chemical reaction on unsteady MHD dissipative Darcy–Forchheimer squeezed flow of Casson fluid over horizontal channel," *Scientific reports*, vol. 13, no. 1, p. 2666, 2023.

[19] K. Sudarmozhi, D. Iranian, I. Khan, J. Alzahrani, A. Al-johani and S. Eldin, "Double diffusion in a porous medium of MHD Maxwell fluid with thermal radiation, heat generation and chemical reaction," *Case Studies in Thermal Engineering*, vol. 43, p. 102700, 2023.

[20] M. Nazeer, S. Saleem, F. Hussain and M. Rafiq, "Numerical solution of gyrotactic microorganism flow of nanofluid over a Riga plate with the characteristic of chemical reaction and convective condition," *Waves in Random and Complex Media*, pp. 1-23, 2022.

[21] A. Ramar, A. Arulmozhi, S. Balamuralitharan, I. Khan, F. Hajjej, M. Khuthaylah and A. Singh, "Melting heat effect in MHD flow of maxwell fluid with zero mass flux," *Case studies in Thermal Engineering*, vol. 53, p. 103910, 2024.

[22] G. Ramasekhar, M. Jawad, A. Divya, S. Jakeer, H. Ghazwani, M. Almutiri, A. Hendy and M. Ali, "Heat transfer exploration for bioconvected tangent hyperbolic nanofluid flow with activation energy and joule heating induced by Riga plate," *Case Studies in Thermal Engineering*, vol. 55, p. 104100, 2024.

[23] K. Sudarmozhi, D. Iranian, H. Alhazmi, I. Khan, A. Chandulal, A. Aljohani, A. Omer and A. Singh, "Effect of heat generation and activation energy on MHD maxwell fluid with multiple slips," *Case Studies in Thermal Engineering*, vol. 59, p. 104424, 2024.

[24] A. Ali, M. Aslam, M. Junaid, T. Sohail, S. Saeed, A. Al-Zubaidi and Z. Mufti, "A comparative analysis of Darcy–Forchheimer nanofluid flow with thermal and solutal effects over a Riga plate," *Journal of Thermal Analysis and Calorimetry*, pp. 1-19, 2025.

[25] H. Alrihieli, M. Aldhabani, E. Alshaban and A. Alatawi, "Thermal-hydrodynamic analysis of a Maxwell fluid with controlled heat/mass transfer over a Riga plate: A numerical study with engineering applications," *Results in Engineering*, p. 104801, 2025.

International Research Journal of Innovations in Engineering and Technology (IRJIET)

ISSN (online): 2581-3048

Volume 9, Issue 6, pp 42-62, June-2025

https://doi.org/10.47001/IRJIET/2025.906007

Citation of this Article:

Shyam Manohar Suthar, & Dr. Shweta Bohra. (2025). Studying Effect of Activation Energy and Chemical Reaction with Heat and Mass Transfer of Maxwell Fluid on Riga Plate Embedded in Porous Media. *International Research Journal of Innovations in Engineering and Technology - IRJIET*, 9(6), 42-62. Article DOI https://doi.org/10.47001/IRJIET/2025.906007

****

